Electrical studies and plasma characterization of an atmospheric pressure plasma jet operated at low frequency

L. Giuliani, M. Xaubet, D. Grondona, F. Minotti, and H. Kelly

Citation: Phys. Plasmas **20**, 063505 (2013); doi: 10.1063/1.4812463
View online: http://dx.doi.org/10.1063/1.4812463
View Table of Contents: http://pop.aip.org/resource/1/PHPAEN/v20/i6
Published by the AIP Publishing LLC.

Electrical studies and plasma characterization of an atmospheric pressure plasma jet operated at low frequency

L. Giuliani, M. Xaubet, D. Grondona, F. Minotti, and H. Kelly
Departamento de Física, Facultad de Ciencias Exactas y Naturales, Universidad de Buenos Aires, C1428EHA Buenos Aires, Argentina and Instituto de Física del Plasma (INFIP), Consejo Nacional de Investigaciones Científicas y Técnicas (CONICET), Universidad de Buenos Aires (UBA), C1428EHA Buenos Aires, Argentina

(Received 18 April 2013; accepted 29 May 2013; published online 27 June 2013)

Low-temperature, high-pressure plasma jets have an extensive use in medical and biological applications. Much work has been devoted to study these applications while comparatively fewer studies appear to be directed to the discharge itself. In this work, in order to better understand the kind of electrical discharge and the plasma states existing in those devices, a study of the electrical characteristics of a typical plasma jet, operated at atmospheric pressure, using either air or argon, is reported. It is found that the experimentally determined electrical characteristics are consistent with the model of a thermal arc discharge, with a highly collisional cathode sheet. The only exception is the case of argon at the smallest electrode separation studied, around 1 mm in which case the discharge is better modeled as either a non-thermal arc or a high-pressure glow. Also, variations of the electrical behavior at different gas flow rates are interpreted, consistently with the arc model, in terms of the development of fluid turbulence in the external jet. © *2013 AIP Publishing LLC*.
[http://dx.doi.org/10.1063/1.4812463]

I. INTRODUCTION

A very active branch in plasma physics is the development of plasma sources able to provide energetic electrons, which produce in turn ions and highly active chemical reactive species, at relatively low gas temperatures. This is motivated by the large number of applications these sources have in plasma biology and plasma medicine, such as pathogen deactivation, wound disinfection, stopping of bleeding without damage of healthy tissue, acceleration of wound healing, control of bio-film proliferation, etc. (see Ref. 1 and references therein).

Among different kind of sources, atmospheric pressure, low-current, low-temperature plasma jets are playing an increasing role also in various plasma processing applications, because they provide plasmas without spatial confinement.[2–4] The basic geometrical scheme of a low-current plasma jet is similar to that employed in the generation of a high-current plasma torch: an electrical discharge is generated in an enclosed region while a relatively large gas flow is sent into the discharge, thus "blowing" the plasma to an outer region, usually unconfined space. Thus, a neutral plasma plume is formed containing ions, electrons, and excited reactive species dragged from the discharge region. The main difference between low-temperature jets and plasma torches is the average current circulating in the discharge, which rarely exceeds 0.1 A in these "cold" jets. A variety of plasma jets using a-c or pulsed power sources operating at quite different voltages, frequencies, and pulse widths, and with different working gases have been presented. For instance, Forster *et al.*[5] presented a jet based on a dielectric barrier discharge (DBD) applying high voltage pulses (15 kV amplitude, 600 ns wide at a repetition rate of 25 kHz) and flowing Ar gas at a flow rate of about 4 l/min. The gas reached temperatures up to 100 °C, but the tip of the plume could be touched with bare fingers. Zhang *et al.* reported on a jet similar to that previously mentioned[6] applying voltage pulses with amplitudes in the range 1–15 kV, repetition rate of 15 kHz, and using Ar, He, and N_2 as the operating gases. Plumes as long as 4.5 cm have been obtained using He at a flow velocity of 20 m/s. Laroussi and co-workers developed a handheld device called "plasma pencil."[7,8] The discharge was performed between two disk electrodes with a central coaxial hole and separated by an alumina insulating disk. A voltage generator producing pulses with amplitudes up to 10 kV, variable pulse widths (from 200 ns to d-c), and repetition rates up to 10 kHz were used. Operating the discharge with He and Ar, plume lengths up to 5 cm and a plume gas temperature of 290 °C were reported. Using the previously described pulse voltage generator, Lu and co-workers[9] presented a jet based on a corona-like discharge that could be operated with all kind of gases, including air, the latter option being attractive for economical reasons. Stoffels *et al.* developed a RF plasma jet called the "plasma needle,"[10] which was extensively used in biomedical applications.[11] Among several other plasma jets that have been developed,[12–16] those which employ simple and non-expensive voltage generators are attractive for biological or medical application not requiring a very strict control of the thermal load on the gas carrier. A comprehensive review, which gives a description of different plasma jet configurations and biomedical applications, was recently presented by Park *et al.*[17]

In particular, Li *et al.* presented recently an atmospheric pressure jet driven by an a–c transformer operated at 50 Hz.[18] The sinusoidal jet current (up to 0.2 A peak value) was limited by the impedance of the transformer, without the use of any ballast element. The discharge voltage presented an almost rectangular shape, reaching values of some hundred volts. The authors claimed that this was a glow

discharge, because no current spikes in the current waveform were observed. Also, in a previous work,[19] the authors give an explanation of the electrical waveforms by relating the discharge current and the discharge voltage drop through Ohm law.

In this work, a plasma jet is considered, operated with either air or argon at atmospheric pressure, and driven by a commercial neon-light tube transformer at a frequency of 50 Hz. The discharge geometry follows approximately that presented in Ref. 20. An electrical study of the discharge is presented, together with a theoretical interpretation. The novel contribution of this work is the interpretation of the discharge as a low-current thermal arc in which a relatively large voltage drop occurs mainly in a highly collisional cathode sheath. Also, the possibility of turbulence in the gas flow is considered, and linked to the behavior of some electrical aspects of the discharge that correlate with the flow rate.

II. EXPERIMENTAL SET-UP

A schematic of the experimental device used to produce the atmospheric plasma jet is shown in Fig. 1. This device consists in two electrodes with a hole of 1 mm diameter, through which the gas flows. The two electrodes are made of stainless steel disks of 20 mm diameter and 3 mm thickness attached to the surface of centrally perforated dielectric disks (Teflon) of different thicknesses d. The hole at the center of the dielectric disk is 2 mm in diameter.

The ac power supply is a commercially available transformer for neon light (25 kV, 50 mA, and 50 Hz), which is connected to a variable autotransformer (Variac) to control the operating voltage amplitude V_{op}. Neon light transformers are quite interesting sources for the generation of low current plasma jets, because they provide an intrinsic current limitation of reactive origin (thus avoiding the use of external ballasts in the discharge circuit) combined with a low commercial price.

The electrical characteristics of the discharge and the appearance of the plasma jet were studied varying the applied voltage amplitude and the gas flow rate. The operating gases were air and argon. The compressed gas flow was measured using a flow meter, and was varied up to 17 l/min.

The voltage V between the electrodes was measured using a high voltage probe (1000×) connected to a digital Tektronix oscilloscope (60 Mhz, 1 GS/s), and the current I was inferred from the voltage drop through a 50 Ω resistance (see Fig. 1).

Photographs of the microplasma jet were taken using a 10 Mpixel digital camera (exposure times of 1/8 s) and the microplasma jet average temperature was measured using a k-type thermocouple located inside the plasma jet.

Different electrode separations d were obtained using three dielectric discs of 1.2, 3.3, and 4.6 mm in thickness, when Ar was used. Due to the impossibility of initiating the discharge in air for the largest gap values, only $d = 1.2$ mm was used in this case.

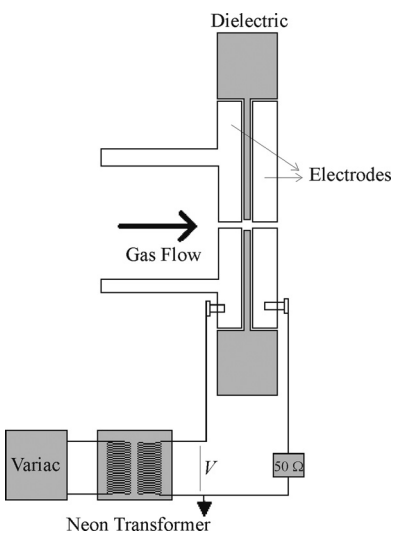

FIG. 1. Schematic of the experimental set-up.

III. EXPERIMENTAL RESULTS

Pictures of the microplasma jet generated with air flow can be seen in Fig. 2. The jet was stable during long periods of time (~30 min) and had typical lengths of 1 cm. Thermocouple measurements showed that the jet was at room temperature and, in fact, it could be touched with a naked finger (see Fig. 2).

Jet photographs for all the investigated range of air flow values are shown in Fig. 3. It can be seen that the length and brightness of the jet depend on the air flow value, and an optimum situation is found for a value of about 10 l/min.

Typical signals of current and voltage taken during the discharge are shown in Fig. 4. The discharge current has a sinusoidal profile with a frequency of 50 Hz, almost independent of the discharge characteristics, since it is controlled by the transformer impedance ((57 ± 1) kΩ). The displacement current, measured with the discharge off, is negligible compared with the discharge current. The voltage signal also has a frequency of 50 Hz, with spikes at the beginning of each cycle corresponding to the zero values of the current. Away from the spikes, the voltage decreases when the current increases and vice versa. This behavior results in a negative slope in the V-I characteristic of the discharge. A similar behavior was observed in the work of Refs. 17 and 18.

Variations in the gas flow did not substantially modify the discharge parameters, the current amplitude (I_{amp}), and the discharge voltage value at the current peak V', remained constant up to around 10 l/min with slight variations for larger flow values (see Fig. 5). For flows larger than

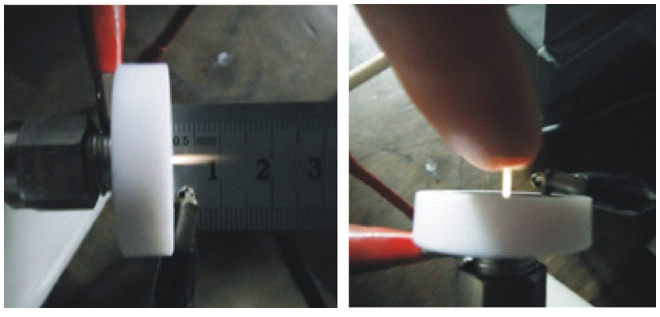

FIG. 2. Images of the atmospheric plasma jet.

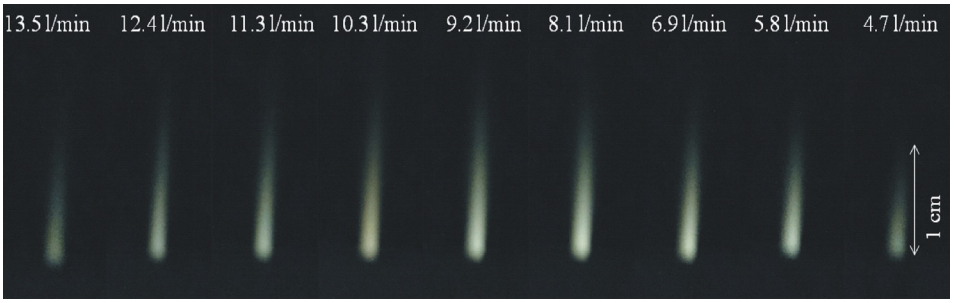

FIG. 3. Jet photographs for the investigated range of air flows.

10 l/min, the current gently decreased, accompanied by an increase in the discharge voltage.

Fig. 6 shows an experimental *I-V* characteristic for $V_{op} = 7.1$ kV, $d = 1.2$ mm, and an air flow of 10 l/min (dots). This characteristic was obtained from the measurements of I and V excluding the very fast current excursion at the initiation of the discharge. The negative slope in the *I-V* characteristic is apparent in this figure, where a theoretically predicted characteristic is also plotted (continuous curve), which will be discussed in Sec. IV.

Fig. 7 shows the voltage profiles of the discharge measured for a flow of argon of 10 l/min and $V_{op} = 4$ kV, for three different electrode separations d. The discharge current (not shown) was the same for the three cases, with an amplitude of 50 mA and with a shape completely similar to that shown in Figure 4. It can be seen that for larger d values the concavity in the voltage signal increases, resulting in characteristics with a more negative slope (see Figure 8).

Finally, Figure 8 shows the results of the *I-V* characteristics for an argon flow rate of 10 l/min and $V_{op} = 4$ kV, for three different electrode separations (dots), together with the model results (curves).

IV. THEORETICAL MODEL

In order to give an interpretation of the measurements, one first notes that for the discharges in air and in argon at the largest separations, the *I-V* characteristics show clear indications of decreasing voltage for increasing current, a

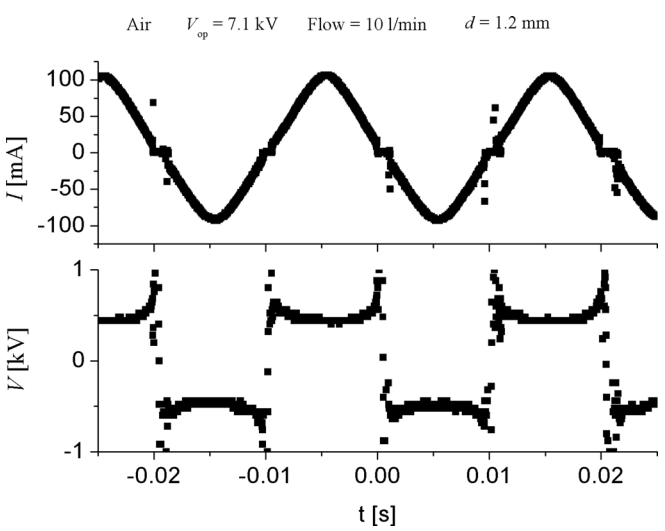

FIG. 4. Typical voltage and current waveforms of the discharge.

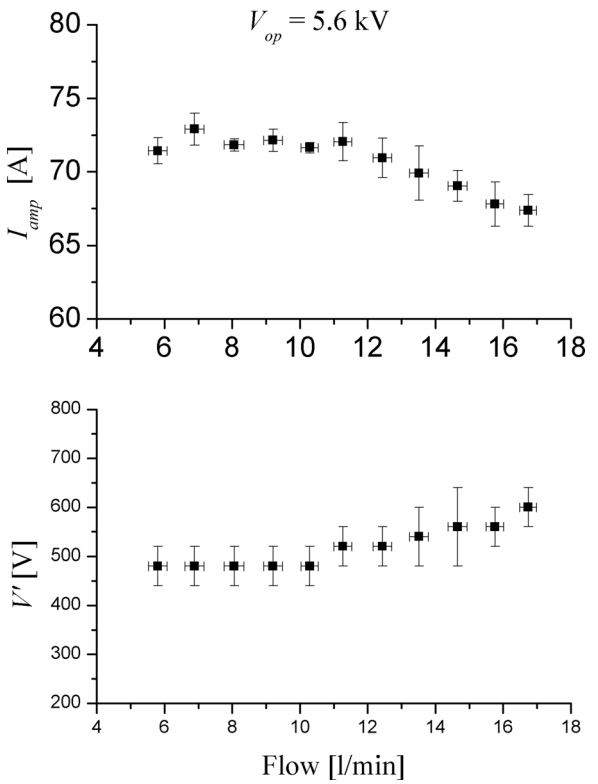

FIG. 5. Current peak value I_{amp} and its corresponding voltage V′ for different air flow rates for $V_{op} = 5.6$ kV.

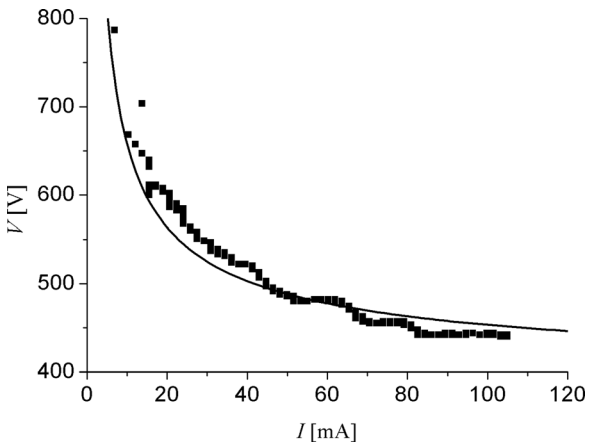

FIG. 6. Experimental (dots) and theoretical (curve) I-V characteristics for air.

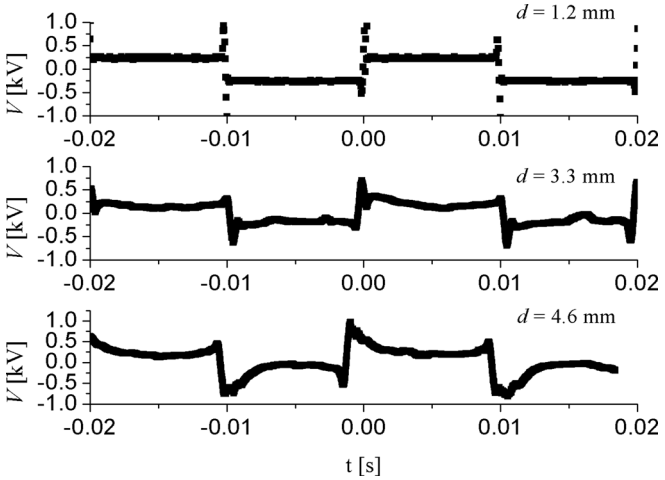

FIG. 7. Voltage profiles of the discharge for a flow of argon of 10 l/min and $V_{op} = 4$ kV, for three different electrode separations.

distinctive feature of arc discharges. So, in order to model this type of discharge, the Elenbaas-Heller equation[21] was solved. This equation states the stationary balance between the Joule heating and the radial thermal conduction at each axial position inside the cylindrical plasma channel separating the electrodes

$$\frac{1}{r}\frac{d}{dr}\left[r\lambda(T)\frac{dT}{dr}\right] + \sigma(T)E^2 = 0, \tag{1}$$

where $T(r)$ is the temperature at each radial position r, $\lambda(T)$ and $\sigma(T)$ are the temperature dependent thermal and electrical conductivities, respectively, and E is the axial electric field, considered to be uniform in the axial section.[21]

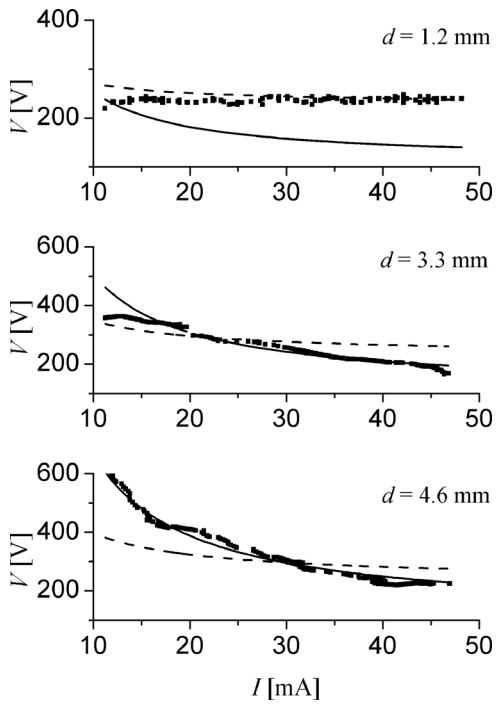

FIG. 8. Experimental (dots) and theoretical I-V characteristics for argon with different electrode separations (full line: thermal arc model and dashed line: non-thermal arc model).

In a thermal arc, all species involved in the processes of electrical and thermal conduction have the same local temperature; whereas in a non-thermal arc, the electrons have a temperature higher than that of the heavy ions and neutrals.[22] The two possibilities were considered in this work. A thermal arc was modeled using tabulated values of the conductivities of air and argon as functions of the temperature, calculated assuming thermal equilibrium.[22] A non-thermal arc was modeled by the same Eq. (1), but considering that the temperature corresponds to the electron temperature, and expressing the thermal conductivity as that corresponding to the gas at a given temperature (gas temperatures up to 1000 K were explored). The contribution of the electrons to the thermal conductivity was included as well, but it was found to be negligible in all cases.[22] As a result, it was not possible to reproduce the measured *I-V* characteristics using the model of a non-thermal arc, which resulted in much flatter characteristics than the measured ones, the only exception being the case of the discharge in argon at the smallest electrode separation. The thermal arc model, on the other hand, reproduced remarkably well those measurements. For this reason, only the thermal arc model will be presented (the results of the non-thermal arc model will be shown for the case of the discharge in argon).

Equation (1) was numerically solved for different values of the temperature at the axis ($r = 0$), where the radial derivative of the temperature is zero, choosing the value of E for which the temperature reaches a value close to the ambient temperature at the channel radius r_c (the precise value of the temperature at this point is not important as long as it is low enough, because the electrical conductivities are negligible below 2000°K). In this way, for each value of the axial temperature, the radial profile of the temperature and the axial electric field are determined, and the current I across the section results from Ohm law as

$$I = 2\pi E\int_0^{r_c}\sigma[T(r)]rdr. \tag{2}$$

In general, the higher the temperature at the axis, the higher is the current. In air, the temperature at the axis ranged from 4000 K, when the current was 20 mA, to 5000 K for currents around 80 mA. In argon, the temperatures were 5000 K for currents of 10 mA, and 6300 K for 50 mA. As an example, in the case of air with a central temperature of 5000 K, the corresponding electric field was $E = 6.05 \times 10^4$ Vm^{-1}, and the current $I = 83$ mA. In Fig. 9, the temperature and the axial current density profiles are shown for this case. As a consequence of the strong dependence of the electrical conductivity with the temperature, the current is concentrated in a central region of radius about one third of the channel radius r_c. In the case of argon, the same value of the current, $I = 83$ mA, corresponded to a central temperature of 6500 K, with $E = 1.90 \times 10^4$ Vm^{-1}. The temperature and current density profiles for this case are shown in Fig. 10.

The voltage drop in the arc is evaluated as $V = Ed_{arc}$, where d_{arc} is the arc length. Assuming a cathode sheath much thinner than the electrodes separation d (which is afterwards verified), $d_{arc} = d$ was considered. In this way, each

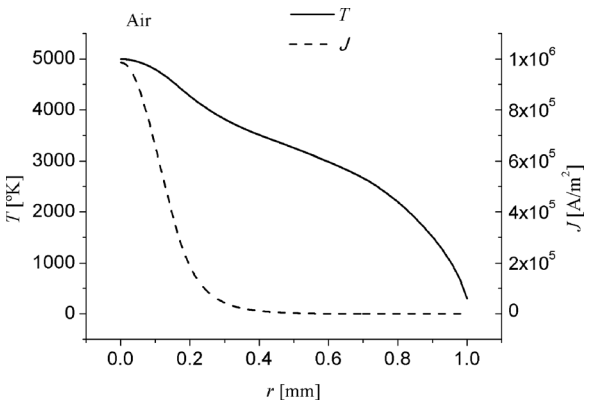

FIG. 9. Temperature and axial current density radial profiles for air for a total current I =83 mA.

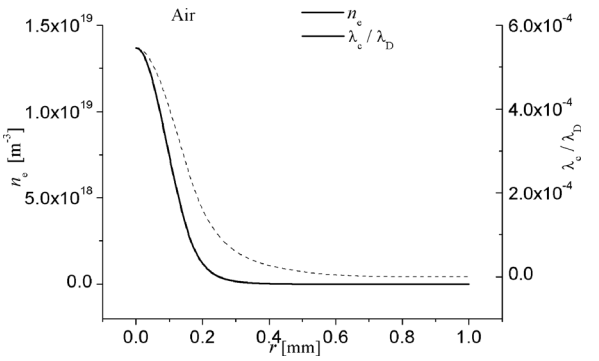

FIG. 11. Electron density and ratio of ion collision mean free path to Debye length, as functions of the radius for the arc in air, with total current I =83 mA.

pair of values (I,V), for given gas and electrodes separation, was parametrized by the temperature at the axis of the arc, and the I-V characteristic of the arc was thus obtained.

To model the experimental characteristics shown in Figs. 6 and 8, the voltage drop in the cathode sheath must be added to that of the arc. A point worth noting is that a single value of the sheath voltage was used for each gas, independent of electrode separation and of the current (110 V for argon and 400 V for air).

The relatively high values of the sheath voltage could be interpreted as due to the high collisionality of the ions in the sheath,[23] together with the low ionization degree of the plasma. The high collisionality in the sheath is a consequence of the high gas pressure (giving a short ion mean free path) and the relatively low current, which produces experimentally determined plasma densities[24,25] not larger than $10^{20}\,\mathrm{m}^{-3}$ for these jets. Using the obtained profiles of temperature, the plasma density can be obtained considering ions to be single ionized so that, from Saha equilibrium, the electron number density n_e contributed by a given neutral species can be expressed in terms of the local neutral density n_A as[22]

$$n_e^2 = n_A S_A(T), \tag{3}$$

where $S_A(T)$ is the temperature dependent Saha factor for the particular neutral species considered. Assuming a uniform pressure close to the standard pressure value, n_A can be written as

$$n_A = n_{0A} T/T_0, \tag{4}$$

with n_{0A} the neutral density corresponding to the standard values of temperature T_0 and of pressure.

With the total electron density contributed by all species, the collisional mean free path of ions, λ_c, and the Debye length, λ_D, can be evaluated. The collisional mean free path turned out to be smaller than the Debye length, the latter being of the order of a few μm. In Fig. 11, the profile of the electron density and that of the ratio of the ion collisional mean free path to the Debye length are shown, for the case of air with a central temperature of 5000 K. Fig 12 shows the profiles of the same magnitudes for argon with a central temperature of 6500 K. The ratio of both lengths is very small in all regions of the arc, indicating highly collisional sheaths. Also, the argon has ratios systematically larger than those of air, which is consistent with a larger collisionality in air and a correspondingly larger sheath voltage drop.

Finally, in order to understand the behavior shown in Fig. 5 of the peak current (and corresponding voltage) with the air flow rate, certain fluid aspects of the discharge should be considered. First, note that the behavior of peak current and voltage correlates with that of the jet length in air, shown in Fig. 3, where the maximum length is reached for values of the flow rate at which the peak current starts to decrease. For both air and argon, the Reynolds number, based on the scale

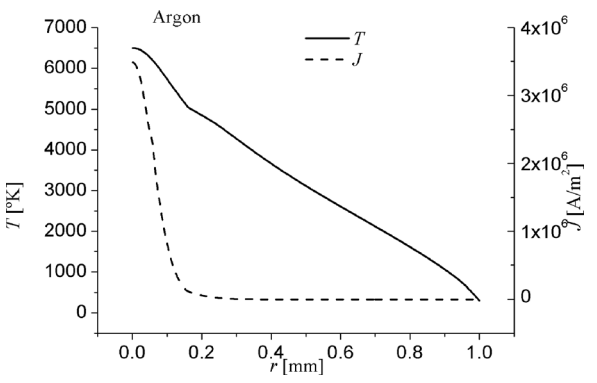

FIG. 10. Temperature and axial current density radial profiles for argon for a total current I =83 mA.

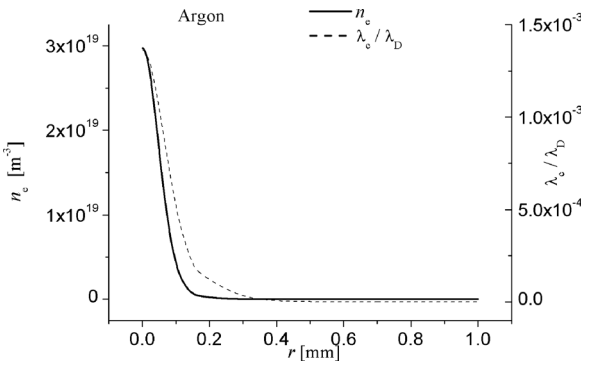

FIG. 12. Electron density and ratio of ion collision mean free path to Debye length, as functions of the radius for the arc in argon, with total current I =83 mA.

length given by the electrode hole diameter, ranges from about 4.0×10^3 to 1.2×10^4 for the flow rates used in this work. Even at the largest flow rates, turbulence is not likely to develop in the region between the electrodes because the entrance length for turbulence development is about 20 diameters[24] for Reynolds numbers about 10^4, which corresponds to a length of about 2 cm, much larger than the device itself. On the other hand, for free shear flows, as is the case of the emerging jet, the transition to turbulence occurs around Reynolds numbers,[25] based also on the hole diameter, of value 10^4, which lies inside the range of Reynolds numbers studied. It is then interesting to note that the transition in the behavior of the current and voltage shown in Fig. 5 occurs when the flow rate is around 10 l/min, corresponding to a Reynolds number about 9×10^3, also coinciding with the maximum length of the external jet, as shown in Fig. 3.

V. DISCUSSION

The first interesting point worth mentioning is that it was possible to decide between thermal and non-thermal arc models from the information given by the measured *I-V* characteristics, as shown in Fig. 8 for the case of argon. The results of the non-thermal arc model indicate, for a given value of electric current, systematically larger electron temperatures than for the thermal model, thus leading to larger conductivities and correspondingly smaller voltage drops that result in flatter characteristics, very different from those measured in argon at large electrode separations and in air.

Another curious result of the model concerns the high temperatures predicted for a thermal arc, from 4000 K to 5000 K in the case of air and between 5000 K and 6300 K for argon. These high temperatures are mostly localized in the central region of the arc, reaching room temperature at about 1 mm from the axis of the discharge with mass averaged temperatures on the whole cross section of the arc above 2000 K. On the other hand, the measured temperature of the external jet was close to room temperature. Possible explanations for this difference of internal and external temperature are either the cooling effect of the electrodes and entrained external air, or that the arc itself is anchored to the internal areas of the electrodes and the gas circulates around it without blowing it outside.

As mentioned, the thermal arc-collisional sheet model reproduced well the *I-V* characteristics of the discharge in air for $d = 1.2$ mm; while in argon, the same model accounts for the electrical characteristics only for the largest separations. At d about 1.2 mm, the argon characteristic is much flatter than that expected from the model (see Figure 8), more similar to a glow discharge or to a non-thermal arc. To check these possibilities, a numerical simulation of a glow discharge was performed. It included electron impact ionization of argon, secondary emission by ion impact, the energy equation of the electrons, species mobilities and diffusion in the self-consistent electric field, determined using Poisson equation, with kinetic coefficients given by the BOLSIG software.[26] The results showed that a glow discharge could be effectively sustained in argon at atmospheric pressure at $d = 1.2$ mm for the measured inter-electrode voltage, leading to electrical currents similar in magnitude to those measured, whereas this was not possible for the larger separations. On the other hand, the model of a non-thermal arc also reproduced rather well the measured characteristic, as shown in Fig. 8. It was thus not possible at this point to determine which of the two possibilities corresponds to the discharge in argon at small separation. In any case, the question arises of why the discharge in air at the same electrode separation ($d = 1.2$ mm) is well described by a thermal arc model. A possible explanation lies in the fact that the electrical conductivity of argon is many times larger than that of air, at the temperatures of each gas that reproduce the measured electrical characteristics. Thus, to similar currents circulating in both gases correspond different Joule powers, larger in air than in argon. On the other hand, the predicted temperatures for air are lower than for argon. In this way, a larger Joule power together with a lower temperature seems to allow air to reach thermal equilibrium, not possible for argon, at the smallest inter-electrode gap for which the thermal effect of the massive electrodes should be more important.

Finally, considering the behavior of the discharge as the flow rate changes, according to what is shown in Fig. 5, when the flow rate increases above 10 l/m, the amplitude of the current peak decreases, whereas the voltage drop increases. As the external flow is predicted to become turbulent for flow rates above 10 l/m, the mentioned electrical behavior is compatible with an increasingly colder arc, as the flow rate increases, because of a more efficient cooling of the internal plasma due to the turbulence-enhanced mixing[25] with the external air.

VI. FINAL REMARKS

An electrical study of an atmospheric pressure plasma jet was presented, together with its interpretation in terms of a model of the discharge. It was found that a thermal arc model with a highly collisional cathode sheath can account for the *I-V* characteristics of a discharge in air and in argon, in the latter case for electrode separations larger than $d = 1.2$ mm. On the other hand, in argon with $d = 1.2$ mm, the discharge appears to be either a glow or a non-thermal arc. Also, turbulence in the external plasma plume appears to have a direct influence on the internal discharge through the enhanced cooling of the plasma.

ACKNOWLEDGMENTS

This work was supported by grants from the Consejo Nacional de Investigaciones Científicas y Técnicas (CONICET) PIP 11220090100219, Universidad de Buenos Aires (UBA) PID 01/1141 and Agencia Nacional de Promoción Científica y Tecnológica (ANPCyT) PICT 2010 No. 0771.

[1]M. Laroussi, in *Plasma Medicine*, edited by M. Laroussi, M. G. Kong, G. Morfill, and W. Stolz (Cambridge University Press, 2012), Ch. 1.
[2]J. L. Walsh and M. G. Kong, Appl. Phys. Lett. **99**, 081501 (2011).
[3]X. Pei, X. Lu, J. Liu, D. Liu, Y. Yang, K. Ostrikov, P. K. Chu, and Y. Pan, J. Phys. D: Appl. Phys. **45**, 165205 (2012).

[4]W. Yan, Z. J. Han, W. Z. Liu, X. P. Lu, B. T. Phung, and K. Ostrikov, Plasma Chem. Plasma Process **33**, 479 (2013).
[5]S. Forster, C. Mohr, and W. Viol, Surf. Coat. Tecnol. **200**, 827 (2005).
[6]J. Zhang, J. Sun, D. Wang, and X. Wang, Thin Solid Films **506**, 404 (2006).
[7]M. Laroussi and X. Lu, Appl. Phys. Lett. **87**, 113902 (2005).
[8]M. Laroussi, C. Tendero, X. Lu, S. Alla, and W. L. Hynes, Plasma Proc. Polym. **3**, 470 (2006).
[9]X. Lu, Z. Jiang, Q. Xiong, Z. Tang, and Y. Pan, Appl. Phys. Lett. **92**, 151504 (2008).
[10]E. Stoffels, A. J. Flikweert, W. W. Stoffels, and G. M. Kroesen, Plasma Sources Sci. Technol. **11**, 383 (2002).
[11]E. Stoffels, I. E. Kieft, and R. E. J. Sladek, J. Phys. D: Appl. Phys. **36**, 2908 (2003).
[12]X. Lu and M. Laroussi, J. Appl. Phys. **100**, 063302 (2006).
[13]D. Dudek, N. Bibinov, J. Engemann, and P. Awakowicz, J. Phys. D: Appl. Phys. **40**, 7367 (2007).
[14]X. Lu, Z. Jiang, Q. Xiong, Z. Tang, and Y. Pan, Appl. Phys. Lett. **92**, 081502 (2008).
[15]Q. Xiong, X. Lu, K. Ostrikov, Z. Xiong, Y. Xian, F. Zhou, C. Zou, J. Hu, W. Gong, and Z. Jiang, Phys. Plasmas **16**, 043505 (2009).
[16]J. F. Kolb, A. A. H. Mohamed, R. O. Price, R. J. Swanson, A. Bowman, R. L. Chiavarini, M. Stacey, and K. H. Schoenbach, Appl. Phys. Lett. **92**, 241501 (2008).
[17]G. Y. Park, S. J. Park, M. Y. Choi, I. G. Koo, J. H. Byun, J. W. Hong, J. Y. Sim, G. J. Collins, and J. K. Lee, Plasma Sources Sci. Technol. **21**, 043001 (2012).
[18]X. Li, X. Tao, and Y. Yin, IEEE Trans. Plasma Sci. **37**, 759 (2009).
[19]X. Li, C. Tang, X. Dai, and Y. Yin, Plasma Sci. Technol. **10**, 185 (2008).
[20]Y. Ch. Hong and H. S. Uhm, Appl. Phys. Lett. **89**, 221504 (2006).
[21]Y. P. Raizer, in *Gas Discharge Physics* (Springer Verlag, Berlin, 1991).
[22]M. I. Boulos, P. Fauchais, and E. Pfender, *in Thermal plasmas: Fundamentals and Applications* (Plenum Press, New York, 1994), Vol. 1.
[23]T. E. Sheridan and J. Goree, Phys. Fluids B **3**, 2796 (1991).
[24]M. V. Zagarola and A. J. Smits, J. Fluid Mech. **373**, 33 (1998).
[25]P. E. Dimokatis, J. Fluid Mech. **409**, 69 (2000).
[26]G. J. M. Hagelaar and L. C. Pitchford, Plasma Sources Sci. Technol. **14**, 722 (2005).